

# Testing the Standard Model at the Precision Frontier with the $Q_{\text{weak}}$ Experiment

ROGER D. CARLINI<sup>1</sup>, WILLEM T.H. van OERS<sup>2</sup>, MARK L. PITT<sup>3</sup>, and  
GREGORY R. SMITH<sup>1</sup>

<sup>1</sup>*Thomas Jefferson National Accelerator Facility, Newport News, VA, 23606 USA*

<sup>2</sup>*Department of Physics and Astronomy, University of Manitoba, Winnipeg, Manitoba, R3T2N2 Canada, and  
Science Division, TRIUMF, Vancouver, British Columbia, V6T2A3 Canada*

<sup>3</sup>*Department of Physics, Virginia Polytechnic Institute and State University, Blacksburg, VA, 24061 USA*

## Introduction

The standard model of particle physics (SM) has been wildly successful describing the strong, electromagnetic and weak forces between visible matter. Despite this success, there is a host of phenomena it fails to describe including neutrino oscillations, gravity, dark matter and baryon asymmetry. Something is missing- the theory is not complete. This conviction has compelled physicists to develop ever more-stringent tests in the hope of finding cracks in the SM that could point to where the beyond-the-standard-model (BSM) physics might lie. Direct searches at high-energy colliders have yielded no evidence for some of the most intriguing possibilities like supersymmetry, and have not been able to shed much light on where to look next.

Low-energy indirect tests of the SM at the intensity/precision frontier are complementary to direct searches and have the potential to provide important multi-TeV constraints on possible BSM physics. The downside of this approach is the experiments are extraordinarily challenging and take a long time to perform.

The recently completed  $Q_{\text{weak}}$  experiment [1-4] is one such rare SM test at the intensity/precision frontier (see Figure 1). Its goal was to measure the proton's weak charge  $Q_W^p$ , which is accurately predicted and highly suppressed in the SM. Since this "SM background" is small (suppressed), the effects

of potential new physics should be easier to see. This experiment exploited parity-violation (PV) to isolate the weak interaction with a precision measurement of the asymmetry in the elastic scattering of longitudinally-polarized electrons from unpolarized protons at small four-momentum transfer ( $Q^2$ ). From this asymmetry, the proton's weak charge could be determined for the first time, and compared to the precise prediction of the SM. The weak mixing angle was also determined at small energy scale, and model-independent multi-TeV constraints were placed on BSM physics.

## Measurement of the Asymmetry $A_{ep}$

The  $Q_{\text{weak}}$  experiment was performed with the custom-built apparatus [1] depicted in Figure 2 in experimental Hall C at Jefferson Lab in Newport News, Virginia. Experience acquired over many years performing increasingly-precise measurements of parity-violating (PV) asymmetries in electron-scattering experiments was crucial to the design of this next-generation experiment.

Far more than for most experiments, the quality and intensity of the longitudinally-polarized electron beam was crucial to the successful outcome of the experiment. The beam quality refers to the requirement that the beam position, angle, energy and intensity be independent of the direction of the electron beam polarization (helicity) either parallel or

anti-parallel to its momentum. This polarization direction was reversed up to 960 times per second (as well as at several much slower time-scales), and the magnitude of the polarization (89%) was continuously measured to an accuracy of  $\pm 0.6\%$ . The  $180 \mu\text{A}$  intensity of the polarized beam was substantially higher than had ever been employed before at Jefferson Lab.

The beam was incident on a 34.4 cm-long liquid-hydrogen target. Almost 3 kW of cooling power was required to maintain the target at 20.00 K due to the heat deposited by the passage of the beam through the target, as well as from the hydrogen circulation-pump and the associated viscous heating of the rapidly-flowing hydrogen with the walls of the target vessel. With a measured noise of only 50 ppm per helicity-quartet from density fluctuations near the 960 Hz helicity-reversal frequency, this was the lowest noise and yet also the highest power liquid-hydrogen target in the world.

About half of the 1.149 GeV electrons scattered from the target in the polar angular range of  $7.9 \pm 3$  degrees were accepted by the apparatus into one of eight collimator apertures arrayed in an azimuthally-symmetric pattern about the beam axis. The 7 GHz of scattered electrons accepted by the collimator system were deflected in the toroidal magnetic field of a large resistive magnet with eight coils onto one of eight 2-m-long Cherenkov detectors made of radiation-hard quartz. The integrated current from the photo-multiplier tubes at each end of the quartz detector-bars formed the yield used to determine a beam-helicity-dependent scattering asymmetry:

$$A_{ep} = \frac{\sigma_+ - \sigma_-}{\sigma_+ + \sigma_-},$$

where  $\sigma_{\pm}$  denotes the detected  $\vec{e}p$  elastic scattering cross-section for a given beam helicity. After correcting for various measured backgrounds and systematic effects that were

painstakingly characterized during the experiment, the final result [3] was  $A_{ep} = -226.5 \pm 7.3$  (stat)  $\pm 5.8$  (syst) ppb at  $Q^2 = 0.0248$  (GeV/c) $^2$ .

### Extraction of the weak charge $Q_W^p$

In the forward-angle limit, the asymmetry  $A_{ep}$  measured in the  $Q_{\text{weak}}$  experiment can be very simply related to the proton's weak charge  $Q_W^p$ :

$$A_{ep}/A_0 = Q_W^p + Q^2 B(Q^2, \theta), \quad (1)$$

where  $A_0 = -G_F Q^2 / (4\pi\alpha\sqrt{2})$ . Here,  $Q^2$  is the four-momentum transfer,  $G_F$  is the Fermi coupling constant,  $\alpha$  is the fine structure constant and  $\theta$  is the electron scattering-angle in the laboratory frame. The  $B(Q^2, \theta)$  term accounts for the proton's internal electromagnetic and weak structure. The electromagnetic structure is well known from various phenomenological fits to years of electron-scattering experiments on the nucleon. The proton's weak structure also includes strange (s) quark and axial components (form factors), which are less well known but small in comparison to the electromagnetic piece. At the deliberately low  $Q^2$  chosen for the  $Q_{\text{weak}}$  experiment, the  $Q_W^p$  term in Equation 1 is about three times larger than the  $B(Q^2, \theta)$  term.

If the proton's weak structure is taken from theoretical calculations,  $Q_W^p$  can be derived from the  $A_{ep}$  measured in the  $Q_{\text{weak}}$  experiment alone. Alternatively, asymmetry measurements at higher  $Q^2$  can be used to determine the proton's weak structure in a fit that also includes the  $Q_{\text{weak}}$  asymmetry datum. In that case  $Q_W^p$  is the intercept of the fit to the "reduced" asymmetries  $A_{ep}/A_0$  vs  $Q^2$  in Equation 1, as described in [3, 4]. The fact that the  $Q_{\text{weak}}$  experiment was performed so close to the intercept at  $Q^2 = 0$ , and achieved such exceptional precision means that similar results

are obtained for  $Q_W^p$  and its uncertainty using either the  $Q_{\text{weak}}$  datum alone or in a fit with all other PVES asymmetry experiments. Details of the procedures used to extract  $Q_W^p$  from the measured PV electron-scattering asymmetries are described in [2-4]. The final result was  $Q_W^p = 0.0719(45)$ , which is in excellent agreement with the SM prediction [5]  $Q_W^p(\text{SM}) = 0.0711(2)$ .

### The weak mixing angle $\sin^2\theta_w$

As discussed in Sec. 1, the proton's weak charge can be related to the most fundamental SM parameter associated with the unification of the weak and electromagnetic interactions: the weak mixing angle  $\theta_w$ , also known as the Weinberg angle. This parameter describes how the (unobserved) massless neutral ( $B$  and  $W_{1-3}$ ) Goldstone bosons associated with the spontaneously-broken EW-symmetry mix, and acquire mass through the Higgs mechanism to form the observed spin-1 force carriers of the EW interaction: the massless photon and the massive  $W^\pm$  and  $Z^0$  gauge bosons.

The numerical value of the weak mixing angle is not explicitly predicted in the SM except in terms of other SM parameters such as the masses of the EW force carriers  $M_{W^\pm}$  and  $M_{Z^0}$ . The magnitude of  $\sin^2\theta_w$  can also be expressed in terms of the gauge couplings  $g$  and  $g'$  of the  $SU(2)_L$  and  $U(1)_R$  groups, respectively, associated with the  $SU(2)_L \times U(1)_R$  gauge symmetry of the electroweak interaction. In terms of these couplings,  $\sin^2\hat{\theta}_W = g'^2/(g^2 + g'^2) = 0.23122 \pm 0.00003$  at the  $Z$ -pole, where the notation  $\hat{\theta}_W$  indicates the modified minimal subtraction ( $\overline{MS}$ ) renormalization scheme [6] used for the rest of this article.

As is the case with the coupling constant  $\alpha$  of quantum electrodynamics, the magnitude of  $\sin^2\hat{\theta}_W$  varies with the energy scale. This scale dependence has its origins in the renormalization group equation. Between the energy scale of the  $Q_{\text{weak}}$  experiment ( $Q =$

0.158 GeV) and the  $Z^0$ -pole ( $M_{Z^0} = 91.1876$  GeV),  $\sin^2\hat{\theta}_W$  changes (runs) by  $-3.2\%$ . The running of  $\sin^2\hat{\theta}_W$  has been precisely predicted [6] within the framework of the SM to an uncertainty of only  $\pm 2 \times 10^{-5}$ . Measurements of  $\sin^2\hat{\theta}_W$  at low- $Q$  constitute important tests of this SM prediction. Moreover, SM tests at  $Q^2 \ll M_Z^2$  can be more sensitive to BSM physics like leptoquarks or  $Z'$ 's than SM tests at the  $Z$ -pole where the lack of an interference term between the  $Z^0$  and the new physics reduces the sensitivity.

Figure 4a shows the  $\sin^2\hat{\theta}_W$  obtained from the  $Q_{\text{weak}}$  experiment [3] along with results obtained from other experiments at both low- $Q$  and at the  $Z$ -pole. At low- $Q$  the semi-leptonic  $Q_{\text{weak}}$  result is joined by a result [7, 8] from atomic parity-violation (APV) observed in  $^{133}\text{Cs}$ , as well as a purely leptonic result from  $\vec{e}e$  (Møller) scattering [9]. The predicted running in this low- $Q$  region below the  $u, d$  quark threshold is nearly flat, which leads to the concept of the “weak-charge triad” formed from the  $Q_{\text{weak}}$ , APV, and Møller (E158) results. These three observables are complementary, because they exhibit different sensitivities depending on how possible new physics scenarios couple to electrons and up and down quarks. This is illustrated schematically in Figure 3. The resulting weighted average of these three lowest- $Q$  ( $Q < 1$  GeV) experiments shown in Figure 4 is  $0.23861 \pm 0.00077$  ( $\chi^2/\text{dof} = 1.9$ , p-value = 0.15), which represents a 9.6  $\sigma$  test of the predicted SM running of  $\sin^2\hat{\theta}_W$ .

We note that the authors of [10] have recently reported using new precision data and an alternate technique to determine the vector polarizability  $\beta$  needed to extract the (APV) weak charge of cesium. Their result differs from the currently accepted value of  $\beta$ , which shifts the extracted weak charge of cesium (and thus the corresponding  $\sin^2\hat{\theta}_W$ ) closer to the SM value than shown in Figure 4. This issue

does not affect the weak charge measurements of either the proton or electron.

Two experiments have been performed between the low- $Q$  region and the  $Z$ -pole. One (eDIS) comes from an experiment [11] probing parity-violation in deep-inelastic scattering of polarized-electrons on the deuteron, which does not affect the low- $Q$  average because of its large uncertainty. The other comes from neutrino-nucleus scattering (NuTeV), but we do not consider it here because it does not include important nuclear-physics effects which influence the result by several standard deviations, as pointed out in [12].

At the  $Z$ -pole, Figure 4 shows results from the Tevatron & LHC [5], and from SLC & LEP [13]. In order to compare the results at low- $Q$  with the  $Z$ -pole results in Figure 4b, the low- $Q$  results were scaled up in  $Q$  by the ratio of the predicted running  $\sin^2 \hat{\theta}_W (Z\text{-pole})/\sin^2 \hat{\theta}_W (Q)$ . The agreement of the low- $Q$  average with the running predicted by the SM is excellent ( $< 0.1\sigma$ ). This precise test of the predicted SM running of  $\sin^2 \hat{\theta}_W$  will set the bar for many years to come, although planned experiments (P2 at Mainz [14], and MOLLER at JLab [15]) have the potential to improve this SM test even further.

### Constraints on the Mass Reach $\Lambda$ for BSM Physics

The sensitivity of the  $Q_{\text{weak}}$  experiment to new BSM physics can be explored [16] by considering an additional term  $L^{\text{new}}$  in the relevant part of the PV neutral current Lagrangian  $L^{\text{msrd}} = L^{\text{SM}} + L^{\text{new}}$ . The new physics term  $(g^2/\Lambda^2)h_q$  is characterized by a coupling strength  $g$  and a mass scale  $\Lambda$ . The flavor-mixing angle  $\theta_h = \tan^{-1} N_d/N_u$  characterizes which quark flavors  $h_{u,d}$  the new physics couples to:  $h_u = \cos \theta_h$ ,  $h_d = \sin \theta_h$ . The corresponding SM term in the Lagrangian is just  $(G_F/\sqrt{2})C_{1q}$ , where the  $C_{1q}$

are the vector-quark weak couplings associated with quark  $q$ . Assuming the new physics couples to the proton's valence quarks in the same proportion as in the SM,  $\theta_h = 26.6^\circ$  and each  $L$  is summed over the  $uud$  quarks. This leads to a simple 95% CL expression [3, 4] relating the ratio  $\Lambda/g$  to the measured  $Q_W^p$  result:

$$\Lambda_{\pm}/g = v \sqrt{4\sqrt{5}/(|Q_W^p \pm 1.96\Delta Q_W^p - Q_W^p(\text{SM})|)},$$

where  $v^2 = \sqrt{2}/(2G_F)$ .

Of course we don't know a priori what the coupling strength  $g$  for the new physics is, because we don't know what the new physics might be. However, models for various new physics scenarios postulate different values of  $g$ . Given a value of  $g$ , we can determine the mass reach  $\Lambda$  associated with that coupling and rule out that particular new physics below the mass reach  $\Lambda$  at the 95% CL. The larger the coupling  $g$  is, the higher the mass reach  $\Lambda$  is for the constraint provided by the  $Q_{\text{weak}}$  experiment.

It is usual [16] to use  $g^2 = 4\pi$ , the coupling associated with the hypothetical BSM physics of compositeness, to characterize and compare the mass-reach constraints provided by different experiments. Compositeness postulates that fermions (quarks and leptons) are not the fundamental building blocks of matter, but are composed instead of even more fundamental constituents. With  $g^2 = 4\pi$ , the  $Q_{\text{weak}}$  experiment rules out BSM physics below a mass scale of 26.6 TeV. Figure 5 shows the mass reach constraint  $\Lambda$  provided by the  $Q_{\text{weak}}$  experiment as a function of coupling strength  $g$ . Mass-reach limits for BSM physics associated with compositeness, leptoquarks (which usually assume  $g^2 = 4\pi\alpha$ ), or the more natural [17] scale  $g = 1$  are called out in Figure 5. Leptoquarks are hypothetical particles that arise in SM extensions like grand unified theories and technicolor. They exhibit properties of both leptons and quarks. Future weak charge measurements (P2 for the proton

and MOLLER for the electron) plan to push to even higher mass scales.

## Summary

The very precise  $Q_{\text{weak}}$  experiment at Jefferson Lab measured a non-zero asymmetry in the elastic scattering of longitudinally-polarized electrons from unpolarized protons that arises solely (in the absence of new physics) as a consequence of the parity-violating weak interaction. This measurement led to the first determination of the proton's weak charge- the charge associated with the weak force- which enabled a powerful test of the standard model of particle physics at the intensity/precision frontier. Since the proton's weak charge is highly suppressed in the SM, it's an exquisitely sensitive observable to test the SM and its possible extensions. The  $Q_{\text{weak}}$  result for  $Q_W^p$  was completely consistent with the prediction of the SM. The SM prediction of the running of the weak mixing angle  $\sin^2 \hat{\theta}_W$  was confirmed at the  $6.5 \sigma$  level using the  $Q_{\text{weak}}$  result. Model-independent constraints on new parity violating, four-point contact interaction (ie weak interaction) physics for the proton were provided by the  $Q_{\text{weak}}$  result: such physics beyond the SM was ruled out below a mass scale  $\Lambda$  of 26.6 TeV (95% CL), far beyond what can presently be reached in direct searches with high-energy colliders.

## Acknowledgements

The authors wish to thank their collaborators on the  $Q_{\text{weak}}$  experiment, as well as the staffs of Jefferson Laboratory, TRIUMF and the MIT-Bates laboratory. This work was supported by the US Department of Energy (DOE) Contract number DEAC05-06OR23177, under which Jefferson Science Associates, LLC, operates the Thomas Jefferson National Accelerator Facility. Construction and operating funding for the  $Q_{\text{weak}}$  experiment was provided through the US DOE, the Natural Sciences and

Engineering Research Council of Canada (NSERC), the Canadian Foundation for Innovation (CFI), and the National Science Foundation (NSF) with university matching contributions from the College of William and Mary, Virginia Tech, George Washington University and Louisiana Tech University.

## References

1. T. Allison, et al. (Q<sub>weak</sub> Collaboration), *Nucl. Instrum. Methods A* 781 (2015) 105.
2. D. Androić, et al. (Q<sub>weak</sub> Collaboration), *Phys. Rev. Lett.* 111 (2013) 141803.
3. D. Androić et al. (Q<sub>weak</sub> Collaboration), *Nature* 557 (2018) 207.
4. R. D. Carlini, W. T. H. van Oers, M. L. Pitt, and G. R. Smith, *Annual Review of Nuclear and Particle Science* (2019) 69 (to be published).
5. M. Tanabashi, et al. (Particle Data Group), *Phys. Rev. D* 98 (2018) 030001.
6. J. Erler and R. Ferro-Hernandez, *JHEP* 03 (2018) 196.
7. C. S. Wood, S. C. Bennett, D. Cho, B. P. Masterson, J. L. Roberts, C. E. Tanner, and C. E. Wieman, *Science* 275 (1997) 1759.
8. V. A. Dzuba, J. C. Berengut, V. V. Flambaum, and B. Roberts, *Phys. Rev. Lett.* 109 (2012) 203003.
9. P. L. Anthony, et al. (SLAC E158 Collaboration), *Phys. Rev. Lett.* 95 (2005) 081601.
10. G. Toh, A. Damitz, C. E. Tanner, W. R. Johnson, and D. S. Elliott, *Phys. Rev. Lett.* 123 (2019) 073002.
11. D. Wang et al. (PVDIS), *Nature* 506 (2014) 67.
12. W. Bentz, I. C. Cloet, J. T. Londergan, and A. W. Thomas, *Phys. Lett. B* 693 (2010) 462.
13. J. Erler and S. Su, *Prog. Part. Nucl. Phys.* 71 (2013) 119.
14. N. Berger et al. (P2), *J. Univ. Sci. Tech. China* 46 (2016) 481.
15. J. Benesch et al. (MOLLER) (2014), <https://arxiv.org/abs/1411.4088v2>(2014).
16. J. Erler, C. J. Horowitz, S. Mantry, and P. A. Souder, *Annual Review of Nuclear and Particle Science* 64 (2014) 269.
17. N. Seiberg, *Phys. Lett. B* 318 (1993) 469.

## List of Figures

1. Depiction of the  $Q_{\text{weak}}$  measurement, which exploits parity-violation in  $\vec{e}p$  elastic scattering to access the weak interaction and determine the proton's weak charge. The polarization direction of the incident electrons was reversed many times per second. The relative rate of scattered events corresponding to the two different spin directions was used to construct a scattering asymmetry, which isolates any signal arising solely from the weak interaction- and any potential parity-violating new physics.
2. CAD view of the experiment [1] with shielding enclosures partially open to reveal their interiors. Beam passed from right to left in this picture. The blue structure on the right is the LH2 target scattering-chamber. A lead triple-collimator system (red) sits between the target and the magnet. The 8 toroidal magnet coils in their support structure sit upstream of the partially disassembled detector bunker (yellow & green shielding on the left), which housed the support structures for retractable drift chambers and the 8 quartz Cerenkov-detector bars arrayed symmetrically around the 4-m-high beam axis.
3. This illustration shows the "Weak Charge Triad" of PV measurements and indicates examples of sensitivities to BSM physics that are unique to specific measurements and those that are common to all. The  $Q_{\text{weak}}$  experiment completes this low  $Q^2$  triad by adding a precise measurement of the proton's weak charge to the existing  $^{133}\text{Cs}$  atomic parity violation (APV) and the SLAC E158 Møller electron parity-violation measurements.
4. Running ( $Q$ -evolution) of  $\sin^2 \hat{\theta}_W$ . (a) The weighted average of the 3 low- $Q$  points (blue) is plotted at arbitrary  $Q$ . Planned future experiments are plotted at their proposed  $Q$  (but arbitrary  $\sin^2 \hat{\theta}_W$ ). (b) Summary of the agreement between various  $\sin^2 \hat{\theta}_W$  experiments and the SM prediction. The experiments above the horizontal green line were derived from asymmetries measured at the  $Z$ -boson scale  $M_Z = 91.1884$  GeV. The low- $Q$  experiments below the green line were scaled to the  $Z$ -pole using the predicted running ( $Q$ -dependence) of  $\sin^2 \hat{\theta}_W$ . The weighted average of the low- $Q$  points is also shown.
5. Mass reach from the  $Q_{\text{weak}}$  experiment [3, 4] for parity-violating, semi-leptonic BSM physics (on the proton), as a function of the coupling " $g$ " associated with new physics. Within the framework of possible new physics,  $g$  could range from a small value (corresponding to a weak coupling if the new physics were for example in the form of leptoquarks), to around unity (the so called "natural scale" which is analogous to nominal SM couplings), or a larger value (more analogous to the strong interaction). The couplings associated with leptoquarks ( $g^2 = 4\pi\alpha$ ), the "natural scale" ( $g^2 = 1$ ), and compositeness ( $g^2 = 4\pi$ ) are shown on the plot. Typically the mass reach of different experiments is compared using compositeness, which implies a mass reach of 26.6 TeV for the  $Q_{\text{weak}}$  result.

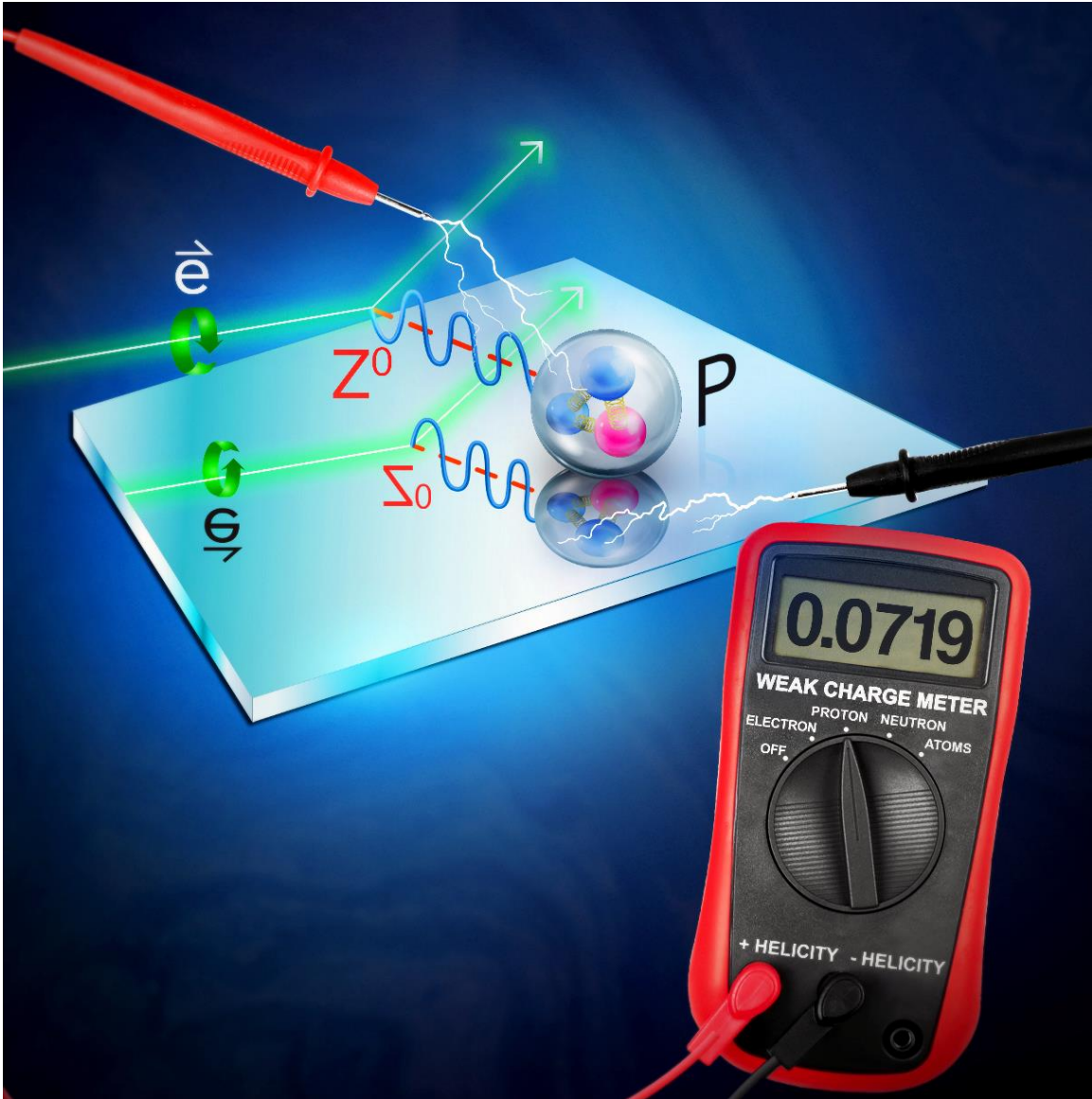


Figure 1. Depiction of the  $Q_{\text{weak}}$  measurement, which exploits parity-violation in  $\vec{e}p$  elastic scattering to access the weak interaction and determine the proton's weak charge. The polarization direction of the incident electrons was reversed many times per second. The relative rate of scattered events corresponding to the two different spin directions was used to construct a scattering asymmetry, which isolates any signal arising solely from the weak interaction- and any potential parity-violating new physics.

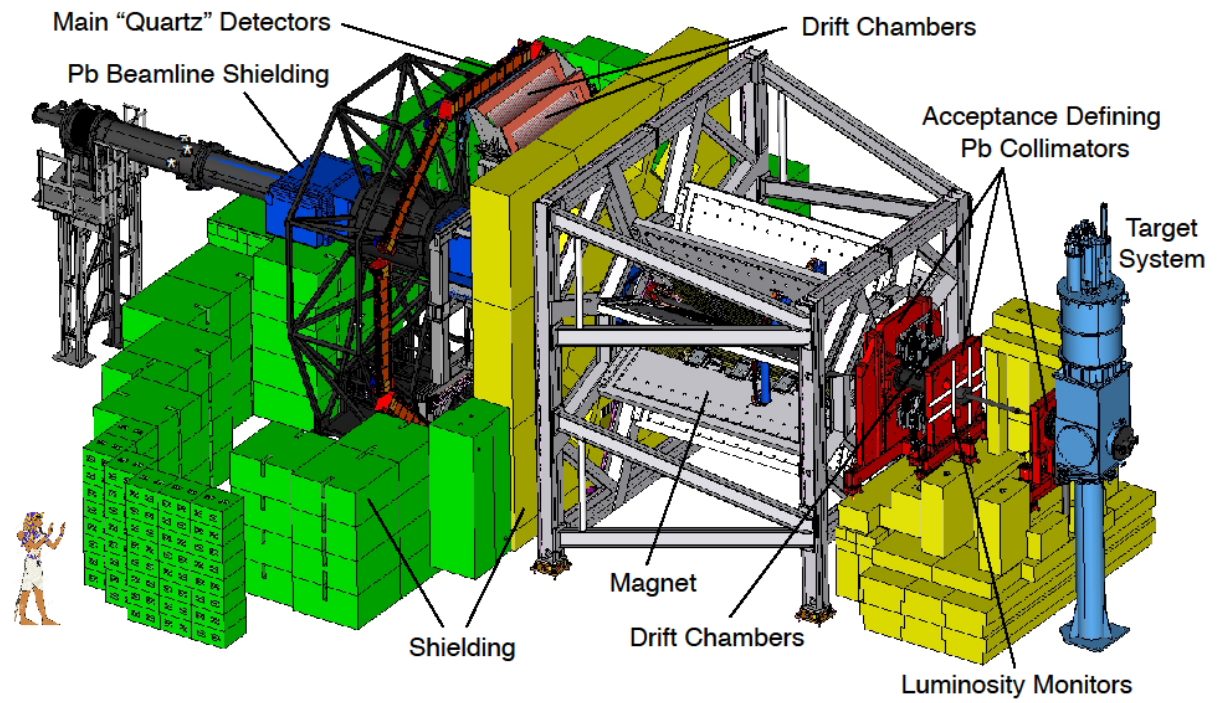


Figure 2. CAD view of the experiment [1] with shielding enclosures partially open to reveal their interiors. Beam passed from right to left in this picture. The blue structure on the right is the LH2 target scattering-chamber. A lead triple-collimator system (red) sits between the target and the magnet. The 8 toroidal magnet coils in their support structure sit upstream of the partially disassembled detector bunker (yellow & green shielding on the left), which housed the support structures for retractable drift chambers and the 8 quartz Cerenkov-detector bars arrayed symmetrically around the 4-m-high beam axis.

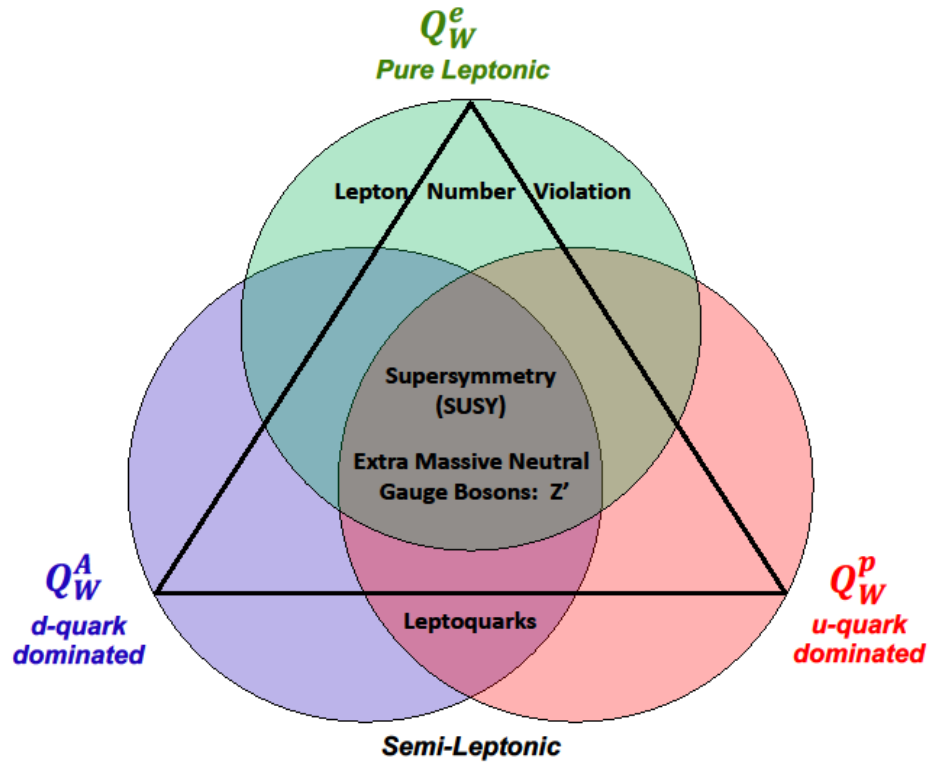


Figure 3. This illustration shows the “Weak Charge Triad” of PV measurements and indicates examples of sensitivities to BSM physics that are unique to specific measurements and those that are common to all. The  $Q_{\text{weak}}$  experiment completes this low  $Q^2$  triad by adding a precise measurement of the proton’s weak charge to the existing  $^{133}\text{Cs}$  atomic parity violation (APV) and the SLAC E158 Møller electron parity-violation measurements.

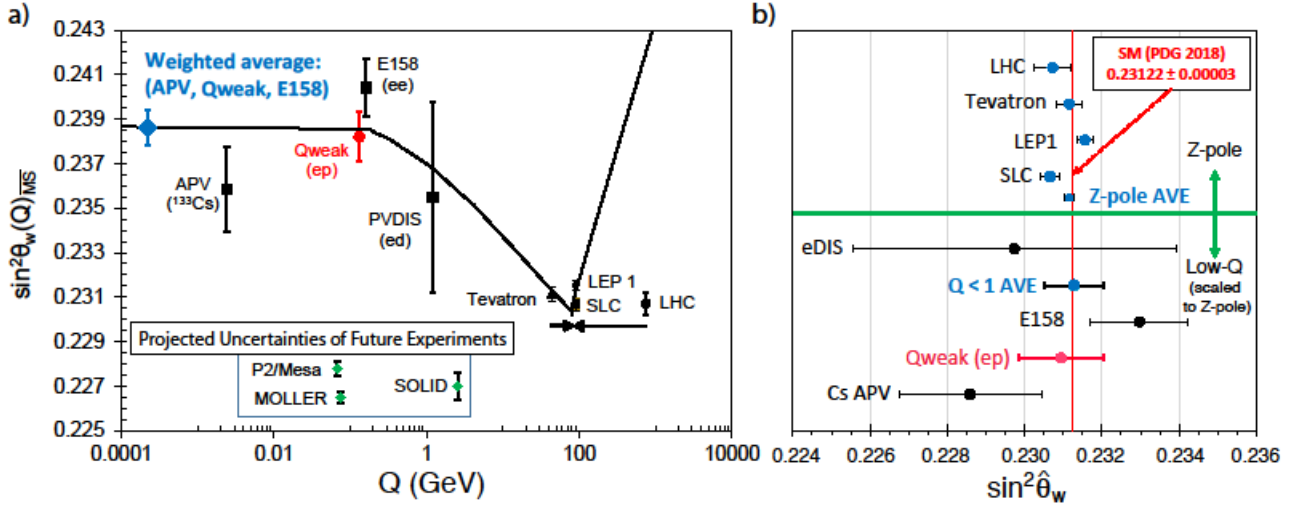


Figure 4. Running ( $Q$ -evolution) of  $\sin^2 \hat{\theta}_W$ . (a) The weighted average of the 3 low- $Q$  points (blue) is plotted at arbitrary  $Q$ . Planned future experiments are plotted at their proposed  $Q$  (but arbitrary  $\sin^2 \hat{\theta}_W$ ). (b) Summary of the agreement between various  $\sin^2 \hat{\theta}_W$  experiments and the SM prediction. The experiments above the horizontal green line were derived from asymmetries measured at the  $Z$ -boson scale  $M_Z = 91.1884$  GeV. The low- $Q$  experiments below the green line were scaled to the  $Z$ -pole using the predicted running ( $Q$ -dependence) of  $\sin^2 \hat{\theta}_W$ . The weighted average of the low- $Q$  points is also shown.

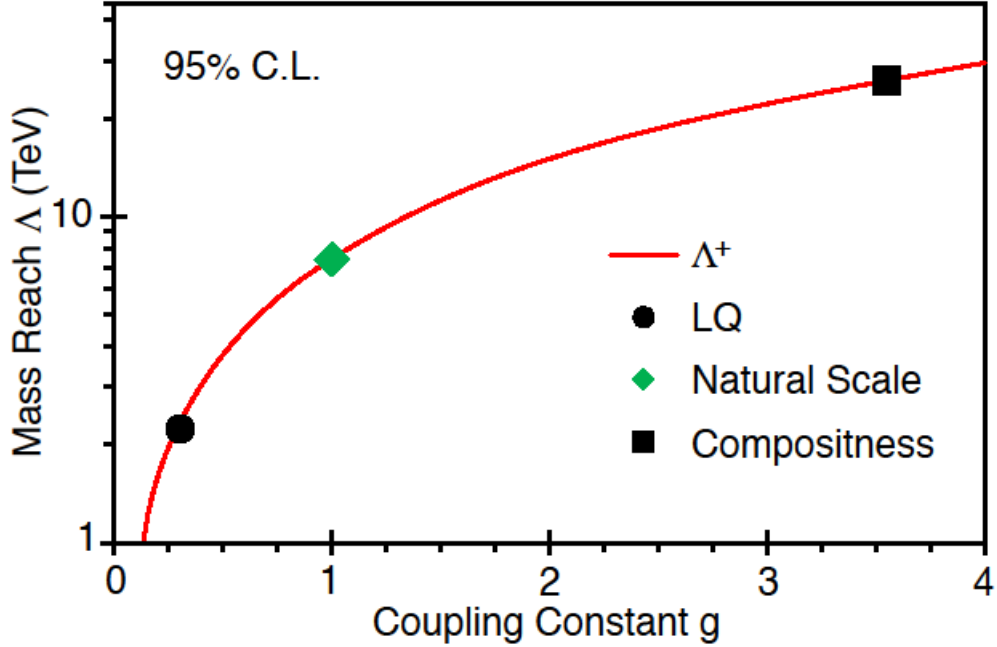


Figure 5. Mass reach from the  $Q_{\text{weak}}$  experiment [3, 4] for parity-violating, semi-leptonic BSM physics (on the proton), as a function of the coupling “ $g$ ” associated with new physics. Within the framework of possible new physics,  $g$  could range from a small value (corresponding to a weak coupling if the new physics were for example in the form of leptoquarks), to around unity (the so called “natural scale” which is analogous to nominal SM couplings), or a larger value (more analogous to the strong interaction). The couplings associated with leptoquarks ( $g^2 = 4\pi\alpha$ ), the “natural scale” ( $g^2 = 1$ ), and compositeness ( $g^2 = 4\pi$ ) are shown on the plot. Typically the mass reach of different experiments is compared using compositeness, which implies a mass reach of 26.6 TeV for the  $Q_{\text{weak}}$  result.

